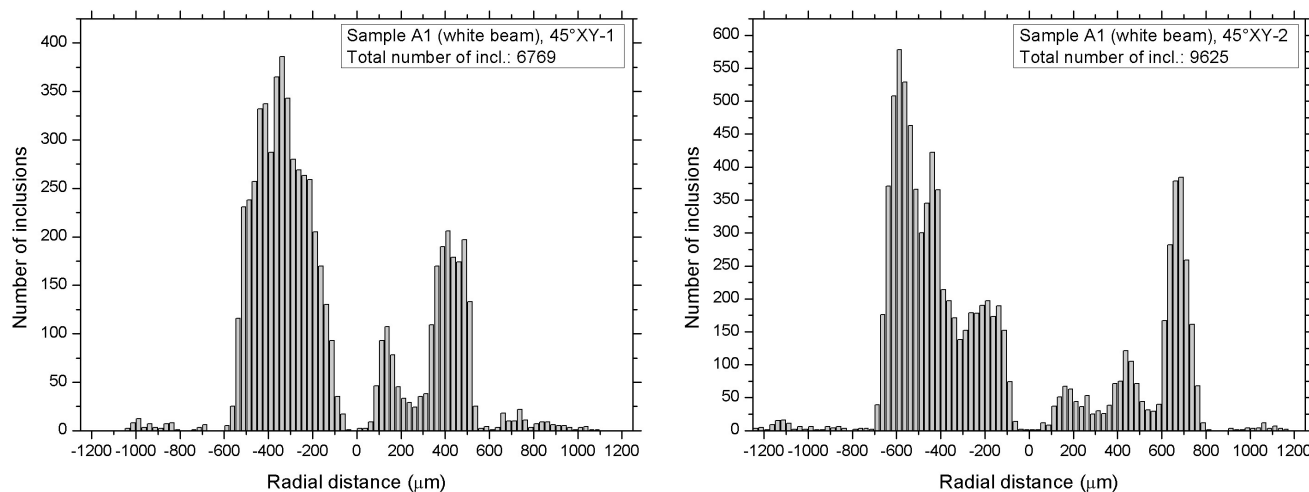
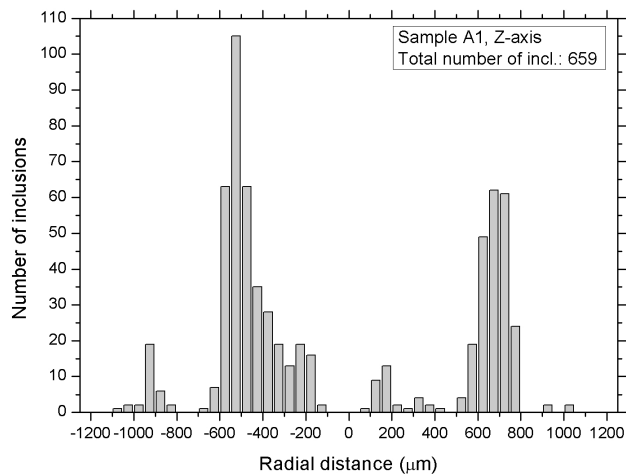
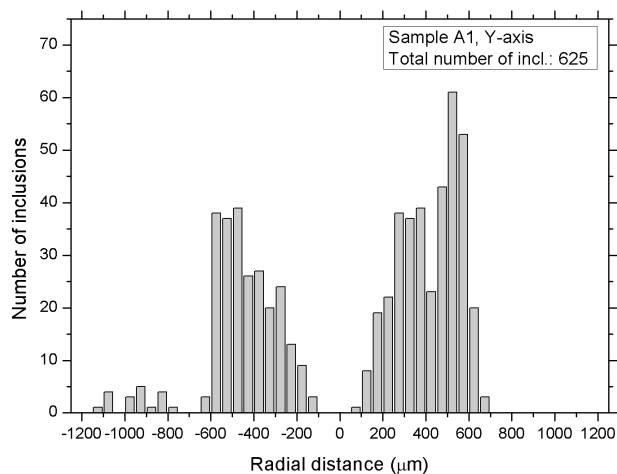
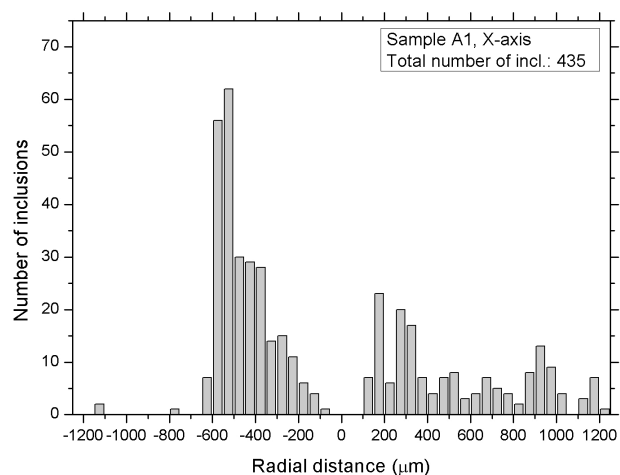
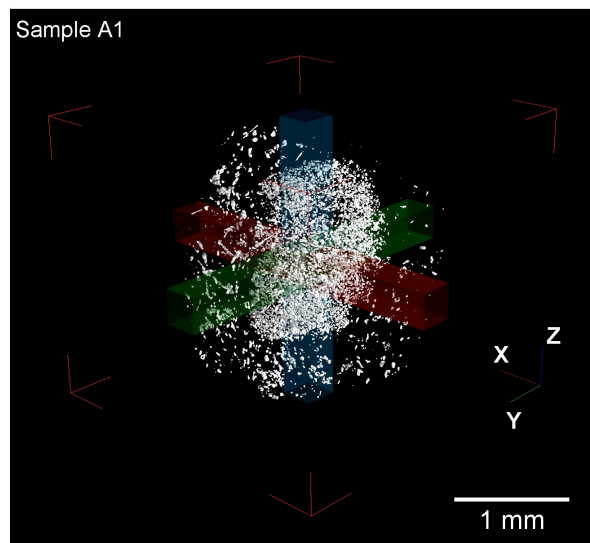


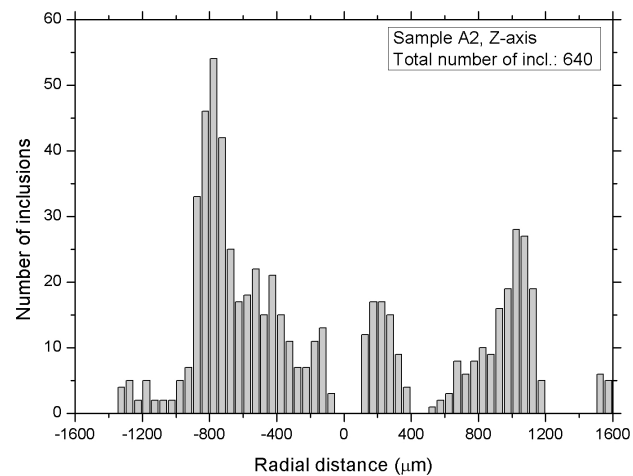
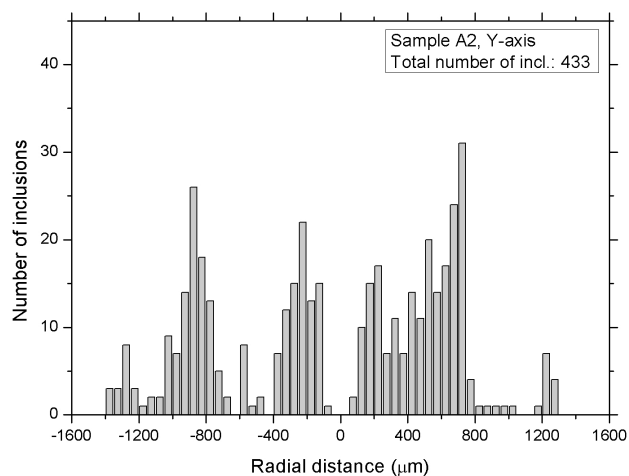
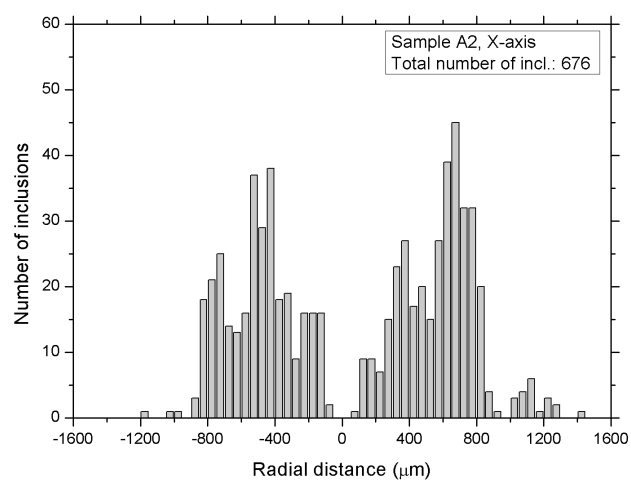
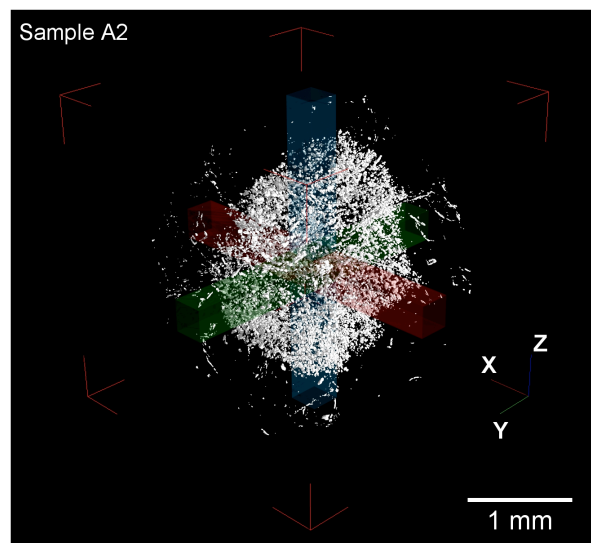
SUPPLEMENTAL FIGURE S1. 3D renderings of garnets A1, B, and C and their melt and fluid inclusions content, obtained from X-ray computed microtomography data sets. Samples A1 and B were analyzed using a synchrotron-based setup whereas sample C was investigated with a cone-beam instrument (TomoLab). The 3D models of sample B allow identifying the coalescence of the main garnet with at least two other smaller crystals in its upper part.



SUPPLEMENTAL FIGURE S2. Additional plots of the distribution of melt and fluid inclusions for sample A1 (white beam mode acquisition), calculated within 300 μm-wide square prisms, oriented along two directions lying in the plane of slice reconstruction (perpendicular to the Z-axis) at 45° from X and Y directions of the data set and passing through the center of inclusion distribution. The results are reported as number of inclusions in each 300\*300\*25 μm<sup>3</sup> sub-domain of each prism.

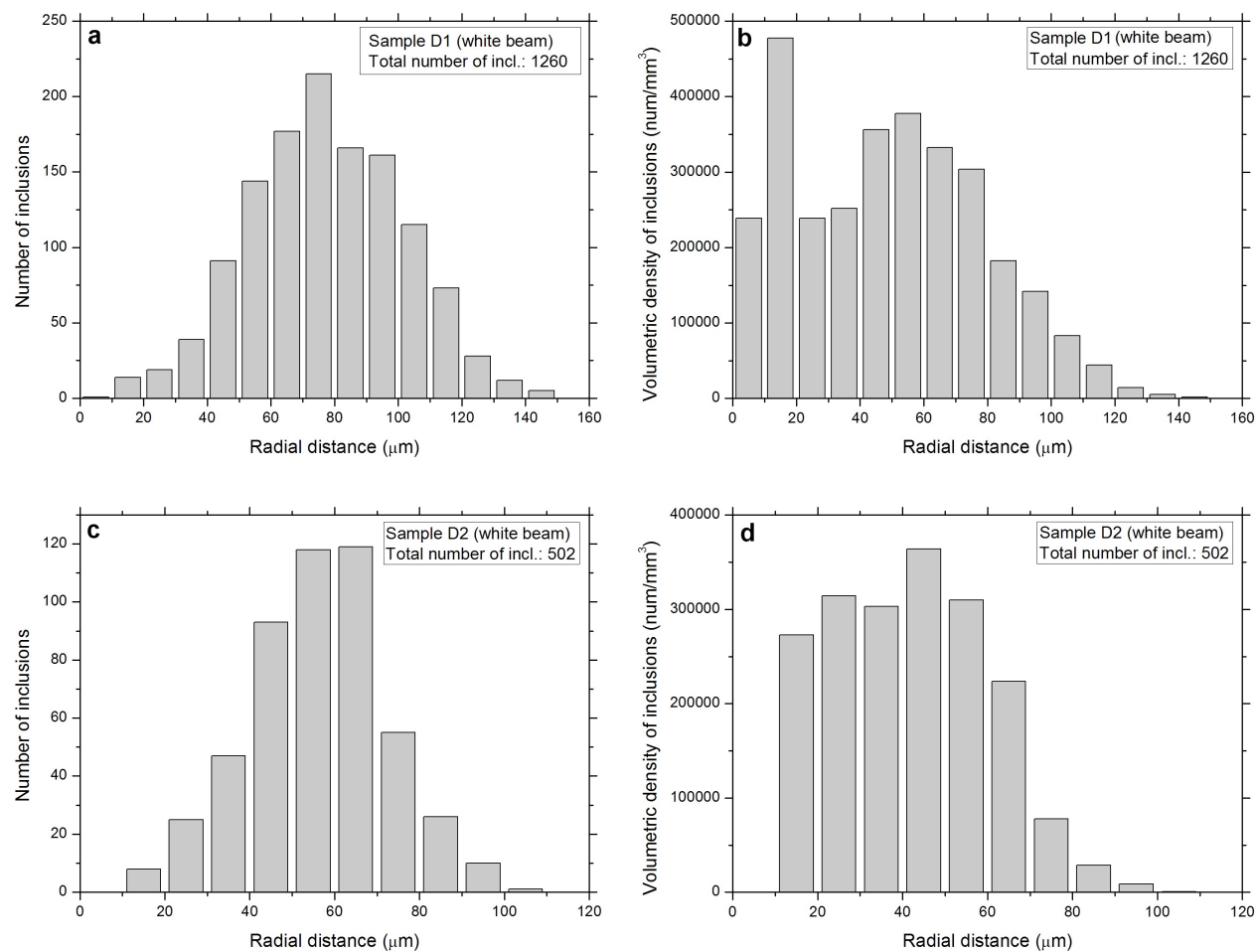


SUPPLEMENTAL FIGURE S3. Distribution of melt and fluid inclusions for samples A1 and A2 acquired in monochromatic beam mode, calculated within  $300\ \mu\text{m}$ -wide square prisms, oriented along the X, Y, and Z directions of the data sets and passing through the center of inclusion distribution. The results are reported as number of inclusions in each  $300 \times 300 \times 50\ \mu\text{m}^3$  sub-domain of each prism. The three semi-transparent prisms are shown together with the entire set of inclusions in the 3D rendering. For sample A1 the orientation of the three mutually orthogonal prisms is not the same in the monochromatic beam data set (shown here) and in the white beam one (Fig. 7).

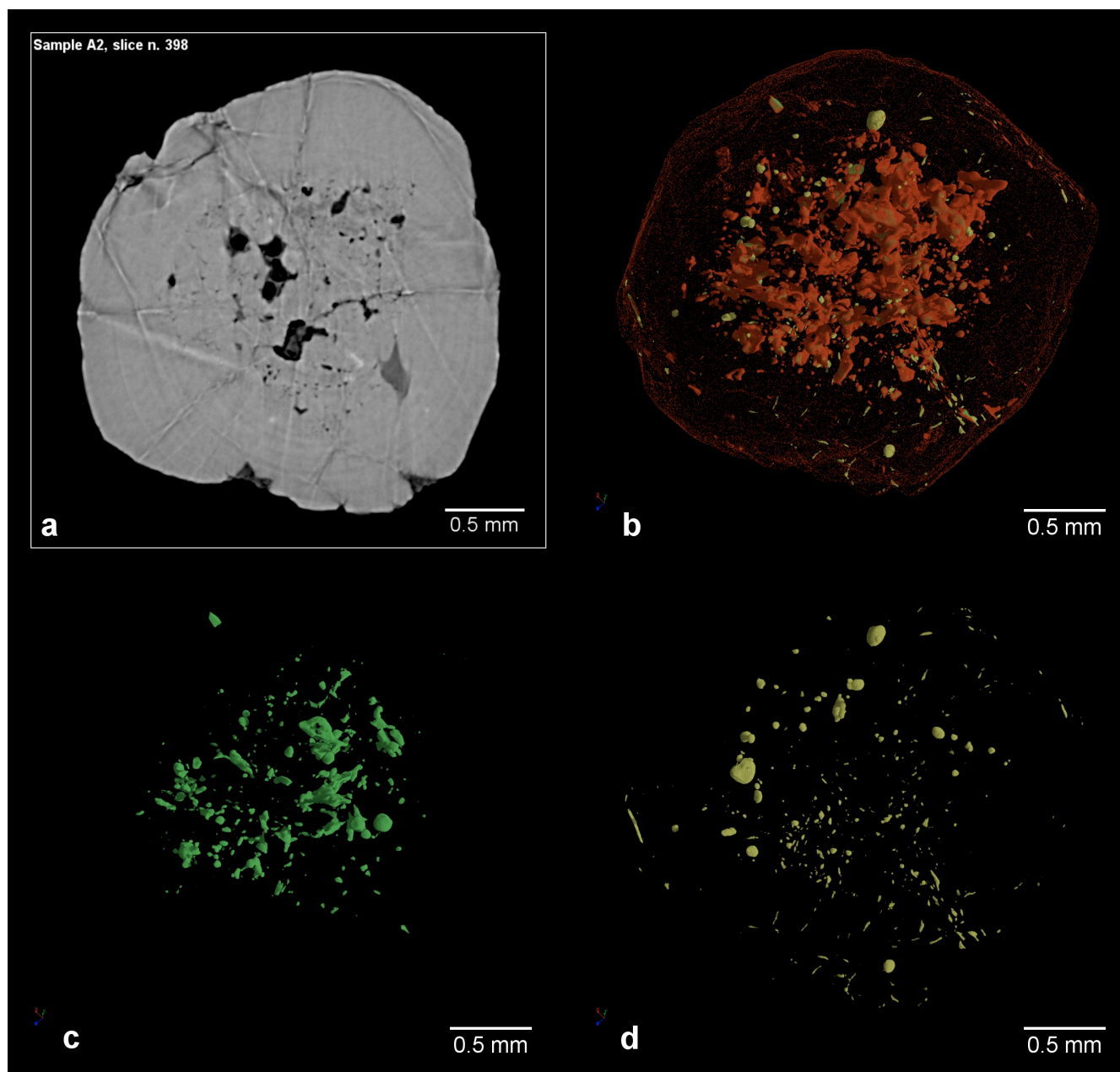


SUPPLEMENTAL FIGURE S3. *Continued.*





SUPPLEMENTAL FIGURE S4. 3D spatial distribution of melt and fluid inclusions (**a**, **c**) and volume inclusions density (**b**, **d**) calculated over concentric spherical shells as a function of radial distance for samples D1 and D2 (Sierra Alpujata). The samples were investigated using the white beam synchrotron setup (polychromatic X-rays). The maximum diameter of samples D1 and D2 is approximately 290  $\mu\text{m}$  and 225  $\mu\text{m}$ , respectively.



SUPPLEMENTAL FIGURE S5. Tomographic 2D slice (**a**) along an almost equatorial plane and 3D renderings of different components of sample A2, after phase-retrieval processing. Melt inclusions are visualized in red together with large crystals of sillimanite and plagioclase (**b**) and with the semi-transparent outer surface of the garnet. Pores, fluid inclusions and some fractures are represented in green (**c**) and heavy mineral inclusions in yellow (**d**).

(see zip file)

#### SUPPLEMENTAL VIDEO S6

3D animation showing in gray values the entire garnet A1 (monochromatic beam data set) and its segmented inner content of melt and fluid inclusions (green-colored) and heavy mineral inclusions (yellow-colored). The VGStudio MAX 2.0 software (Volume Graphics, Germany) was used to create the animation.